JOURNAL OF Applied Polymer SCIENCE

Mechanical and Abrasive Wear Behavior of Glass and Basalt Fabric-Reinforced Epoxy Composites

Chelliah Anand Chairman, Subramani Palani Kumaresh Babu
Department of Metallurgical and Materials Engineering, National Institute of Technology, Tiruchirapalli 620015, India
Correspondence to: Chelliah Anand Chairman (E-mail: mechanand2003@gmail.com)

ABSTRACT: Multipass two-body abrasive wear behavior of basalt and glass fabric-reinforced epoxy composites have been carried out by using a pin-on-disc machine. Basalt and glass fabric-reinforced epoxy composites have been fabricated by hand layup technique. The mechanical properties of basalt and glass fabric reinforced epoxy composites were evaluated. Abrasive wear performance was evaluated at ambient temperature using 400 grade Silicon Carbide paper as a counter face. The elemental compositions of fabricated composites were quantitatively analyzed by using energy dispersive X-ray spectroscopy. The abrading wear mechanisms have also been studied by worn surface analysis using scanning electron microscopy. © 2013 Wiley Periodicals, Inc. J. Appl. Polym. Sci. 130: 120–130, 2013

KEYWORDS: thermosets; microscopy; mechanical properties

Received 3 January 2013; accepted 3 February 2013; published online 8 March 2013
DOI: 10.1002/app.39154

INTRODUCTION

The characteristics of low density, specific strength, and stiffness make polymer-reinforced composites an appropriate material for tribological applications. The tribological performance of fiber-reinforced polymer composites (FRP) is usually related with the properties of their reinforcement. Among the various reinforcements, glass fabric-reinforced composites are generally used in abrasive wear components such as conveyor belt, shuttle, tillage tools, vanes and gears,[1] pumps handling industrial fluids,[2] sewage and abrasive-contaminated water,[3] roll neck bearings in steel mills which are subjected to heat and shock loading, chute liners abraded by coke, coal and mineral ores handling equipment and wind blades.[4] According to American Society for Testing and Materials (ASTM) standard, wear is defined as the damage to a solid surface, generally involving progressive loss of material, due to relative motion between that surface and contacting substance.[5] Types of wear are abrasive, adhesive, erosion, fatigue, and fretting wears. Abrasive wear is the most important among all the forms of wear because it contributes almost 63% of the total cost of wear.[6] Abrasive wear is caused due to hard particles that are forced against and move along a solid surface.[7] In two body abrasion, wear is caused by hard protuberances on one surface which can only slide over the other. According to the recent tribological survey, abrasive wear is responsible for the largest amount of material loss in industrial practice.[8]

More research work has been done to overcome or inhibit the abrading of glass fibers reinforced composites by incorporating fillers into the matrices.[9–16] Recently, Suresha et al. compared the abrasive wear behavior of glass and carbon fabric-reinforced vinyl ester composites. They concluded that carbon fabric is having better wear resistance than glass fabrics.[17] Friedrich investigated the abrasive wear behavior of the epoxy reinforced with carbon, glass and aramid fabrics and reported that aramid fabric is having better wear resistance than glass and carbon.[18] Least attention has been devoted to the carbon fibers in tribological and mass applications due to its high cost.[19] The characteristic restrictions of glass fibers such as bio-degradability, specific durability, and low wear resistance pave a way for finding an alternate material for developing wear resistance polymers. Basalt fiber has been gaining popularity over other fibers due to excellent mechanical properties, high abrasion resistance, and relatively low price. Several works have been executed on the development of modern continuous basalt fibers-reinforced composites for structural applications. Basalt fibers-reinforced composite is the most preferable one, due to its low price in comparison with other types of fibers.[20] Basalt is produced from basic volcanic rock by melt technology without any other additives in a single production process.[21] The next generation inorganic basalt fiber is expected to rival the general-purpose glass fiber.[22] Basalt fibers have been studied extensively as reinforcement for polymer composites and are mainly focused on the polypropylene and epoxy resin.[23–25] Comparison of

mechanical properties and corrosion resistance of basalt fibers over glass fibers has been studied and reported.[26–29] Bin Wei et al.[29] mentioned that basalt fiber-reinforced epoxy composite interfacial property is better than glass fiber-reinforced epoxy composite even after sea water treatment. In this current research, better abrasion resistance was obtained for basalt fiber-reinforced composites than glass fiber-reinforced composites and this is attributed to good interface property of basalt fibers with matrix.

In recent years much research has been devoted to explore the advantages of a thermosetting matrix for composite materials. One such matrix is an epoxy resin which is extensively studied because they exhibit low shrinkage, higher mechanical properties, easy fabrication, excellent chemical and moisture resistance, good wet ability and good electrical characteristics.[30] The mechanical properties and the wear characteristics of the composites, determine its acceptability in tribological applications. In this regard, the aim of the article was to investigate the two-body abrasive wear behavior of basalt and glass fabrics-reinforced epoxy composites. The result reported in this paper has suggested the possibility of replacing glass fibers by basalt fibers in abrasive wear situation. There needs to be some more identification to be observed experimentally to further clarify the potential usability of basalt fibers.

EXPERIMENTAL PROCEDURES

Materials

The basalt plain weave fabrics of 150 g/m^{2}were obtained from Asamer basaltic fibers, Austria. The characteristics and mechanical properties of the basalt fibers as received are given in Table I. Woven E-glass fabric (360 g/m^2) of diameter 10–15 μm were employed. The epoxy matrix investigated is a medium viscosity epoxy resin (LY556) with a density of 1.15–1.20 g/cm^3 and a room temperature curing hardener (HY 951) both supplied by Javanthee Enterprises(Huntsman distributor)-Chennai, India. The composites consist of bi-directional fabric which is plain and symmetrical and their SEM images are shown in Figure 1(a,b).

The composites have been fabricated by using hand layup technique. The manufacturing process involves the mixing of the epoxy resin with the hardener at a ratio of 100:38 (weight basis). Then the catalyzed resin mixtures are spatulated on a 300 × 300 mm^2 mold plate. Precut of reinforcing layer of size 300 × 300 mm is laid on the wet resins of epoxy. Air is worked out by brush dabbing. The reinforced layers are soaked by the resin. Subsequently, eighteen layers are built up to obtain the thickness of 3 ± 0.2 mm. The laminated plates were cured under a pressure of 0.0965 MPa. Finally laminated composites were removed and trimmed to the required size. The specimens required for abrasive studies (5 × 5 × 3 mm^3) were cut from the laminated composites by using diamond tip cutter. After fabrication, the fabric content for composite samples is determined by a resin burn-off test according to the ASTM D3171 specifications. The burn-off experiments were done for the composites to determine the mass content of resin and fiber. Fiber weight fractions of 53.38% and 57.76% were found, respectively, for basalt and glass fabric-reinforced epoxy composites. The wt % fabric (x) is determined from the following formula:

$$x = \frac{w}{w_0} \times 100 \quad (1)$$

w_o and w are the initial weight and weight after the matrix burn-off, respectively. Actual density of the composites specimens was determined using a high precision digital electronic weighing balance of 0.1 mg accuracy by using the Archimedes principle. Void content is calculated from the difference between

Table I. The Properties of the Woven Basalt Fabric (as Received)

Material	Volcanic rock
Basalt fabric	Plain
Yarn linear density (Tex)	50-4800
Monofilament diameter (μm)	10-30
Density (g/cm^3)	2.8
Tensile modulus (GPa)	80-90
Thickness (mm)	0.11
Tensile strength (MPa)	1350-4750

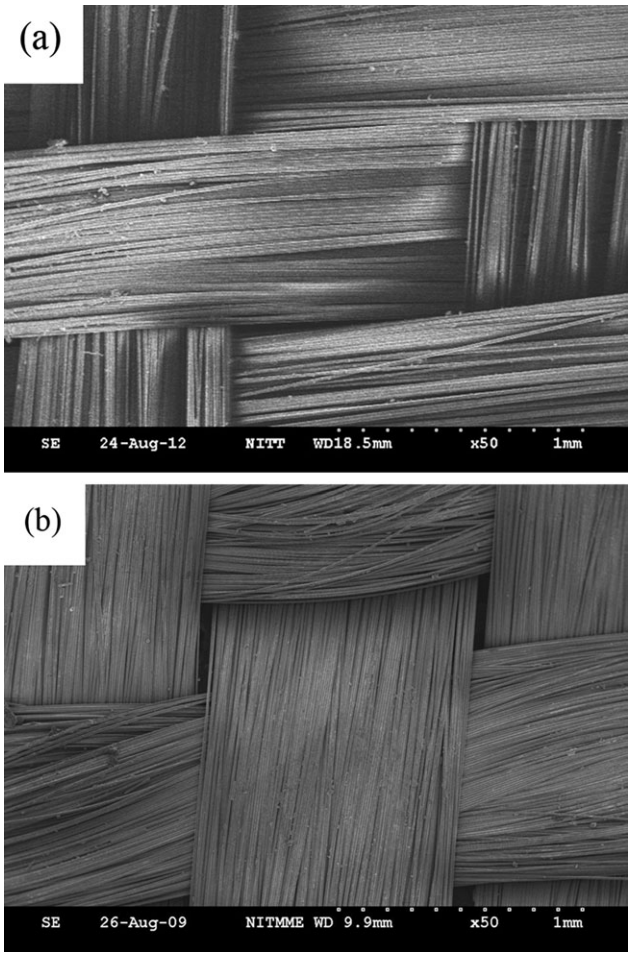

Figure 1. SEM image of woven (a) basalt fabric (b) glass fabric.

Table II. Result of Density and Void Contents for Laminated Composites

Composites	Theoretical density (g/cm^3)	Actual density (g/cm^3)	Void content (%)	Hardness (Shore D)
Glass-Epoxy (Glass-E)	1.67	1.61	3.59	69
Basalt-Epoxy (Basalt-E)	1.76	1.725	1.98	81

theoretical density and actual density. Table II lists the calculated values of the density and void content for the laminated composites.

Abrasive Wear Experiment

The pin-on-disc machine (as per ASTM G-99 standard,) is used for two-body abrasive wear tests (Figure 2).

The test specimens were glued using an adhesive to pins of size 6 mm diameter and 25 mm length. To make uniform contact with the counter surface, the specimens for each test were polished against a 600 grade SiC paper. During the course of the experiment, warp fibers in the sample, are parallel to the abrading direction and the weft fibers are perpendicular to it. The disc and the specimen surfaces were cleaned with a soft paper soaked in acetone and thoroughly dried before the test. The pin assembly was initially weighed to an accuracy of 0.1 mg in an electronic balance. The specimens were abraded against the water proof silicon carbide (SiC) abrasive papers (400) at a constant running speed of 200 rpm in multipass condition. The embedded hard SiC particles abraded the test samples. A constant sliding velocity of 2 m/s and loads of 5, 10, and 15 N were applied. The weight loss measurements were carried out for abrading distances of 25, 50, 75, and 100 m. For each test, experiment was repeated twice and the mean value of weight loss was used for specific wear rate calculations. The specific wear rate (K_s) of the composites was calculated as:

$$K_s = \frac{\Delta V}{L \times d} (\mathrm{m}^3/\mathrm{Nm}) \quad (2)$$

where ΔV is the change in volume loss (m^3) L is the load (N), and d is the abrading distance (m). The worn surface of the composites and abrasive paper were gold sputtered before using a scanning electron microscope. Scanning electron micrographs (SEM) of SiC abrasive paper of grade 400 before the abrasion is shown in Figure 3.

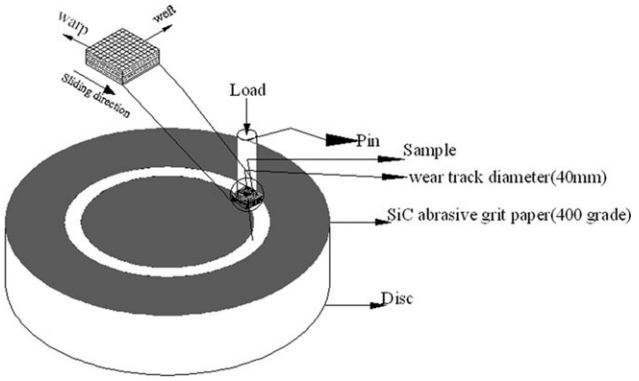

Figure 2. Schematic diagram of pin on disc machine.

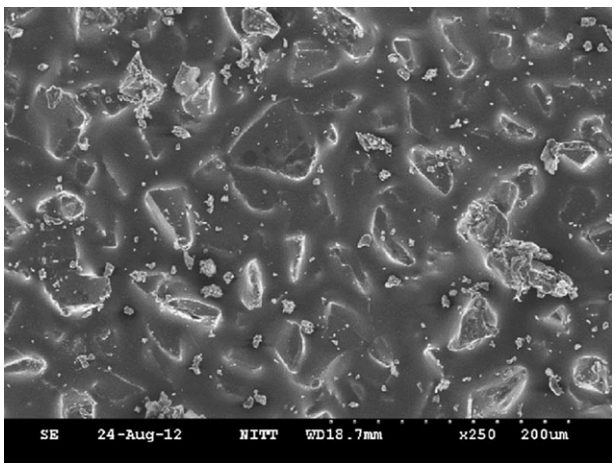

Figure 3. SEM picture of 400 grit SiC paper before abrasion.

Testing of the Mechanical Properties of the Laminated Composites

Tensile test was conducted using a universal testing machine of model UTE- 40 at a cross head speed of 2 mm/min. The tensile experiments were performed according to ASTM standard D3039 using 25.4 mm wide and 250 mm long specimens. A uni-axial load is applied, through both the ends. Five samples were tested for each composites and the average value is taken. The compression tests were conducted according to ASTM D 6641standards. The mechanical properties for compression test were conducted by an Instron 8562 testing machine. Short beam test was used to determine the inter-laminar shear strength (ILSS) of the basalt fiber and glass fiber-reinforced epoxy composites. The test was conducted as per ASTM D2344-84on Lloyd LR-100K machine, span to depth ratio for specimen was 5:1.The surface hardness of the laminated composites was measured using a shore D Durometer (M/s. PSI Sales, India) as per ASTM D 2240 specifications.

RESULTS AND DISCUSSION

Tensile Strength

Figure 4 shows the results of the tensile test for the basalt-E and glass-E composites. It is observed that the basalt fabric type shows an increase of 23% of the tensile strength when compared with the glass fabric-reinforced epoxy composites.

Macroscopic images in Figure 5(a,b) show the fractured surfaces of the glass-E and basalt-E composite systems, respectively. The broken surface of glass fiber shows characteristic of ductile fracture [Figure 5(a)] indicating that adhesion between matrix and fibers play an important role in tensile resistance. The tensile test specimen of basalt-E composites demonstrated no occurrence of failure by shear and/or debonding in the interface between laminates. Fracture surface of basalt-E composite [Figure 5(b)] shows the characteristic of brittle fracture and a

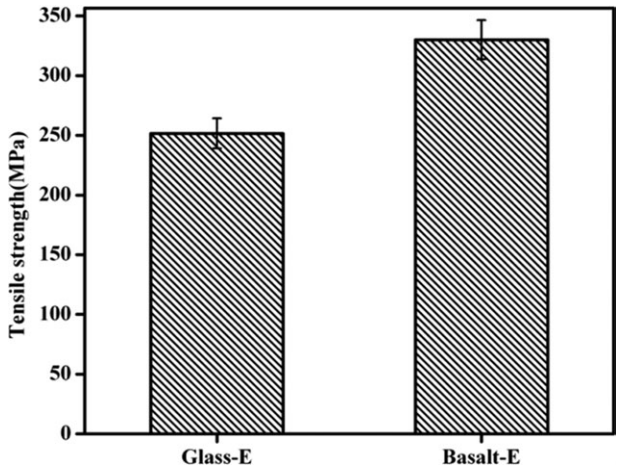

Figure 4. Tensile strength of the laminated composites.

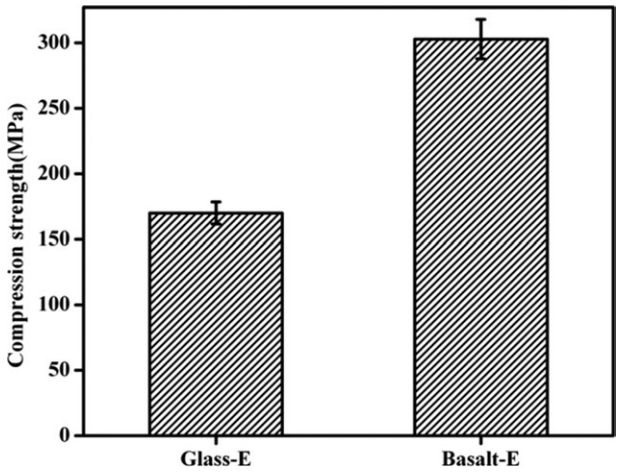

Figure 6. Compression strength of the laminated composites.

little fiber pull-out indicating better fiber-matrix adhesion. Therefore better fiber-matrix adhesion of basalt-E composites has good tensile properties over glass-E composites.

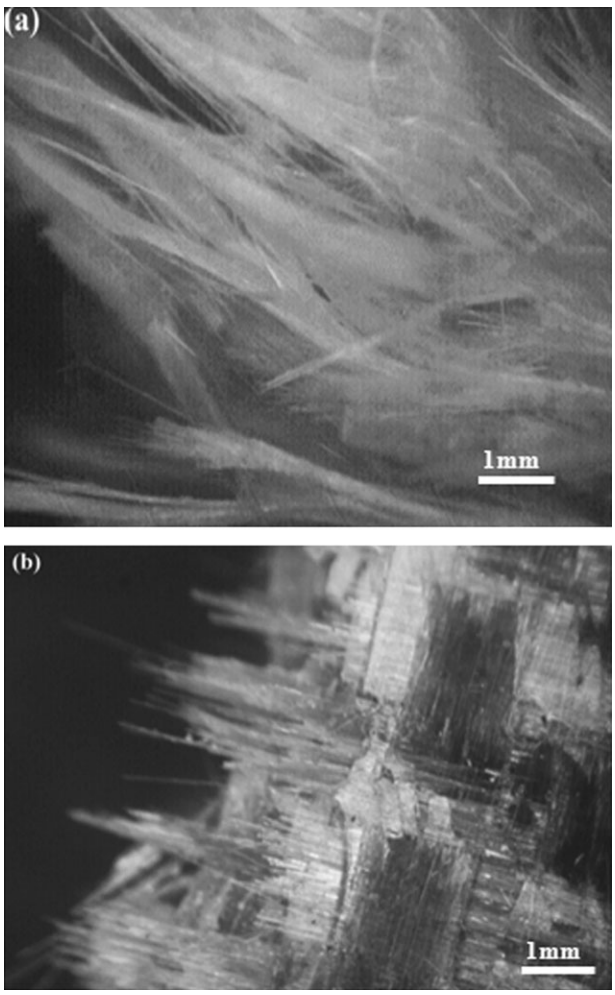

Figure 5. Images showing the fracture surface after tensile testing of the (a) glass-E composite. (b) basalt-E composites.

Compressive Strength

Generally compression induces transverse tension that leads to interface debonding and shear yielding of the matrix between the fabrics [Figure (6)] shows the compression strength of the basalt-E and glass-E composites. Compression strength of basalt-E is 43.8% higher than that of glass-E. The increase in the compressive strength is attributed to the presence of basalt fibers having high hardness. During the compressive test, all components deformed plastically and the hard basalt fibers were pressed into the matrix. The prolonged compression causes the hard fibers to resist the loads and not deform plastically.[31] The rigid bonding between the basalt fibers and epoxy is good enough to transfer the load and endures the superior compression resistance.

The compression failure by micro-buckling in the glass-E composites is due to the damage produced by the plies containing fibers parallel to the load. The micro buckling is characterized in Figure 7 for glass-E composites. Similar trends were observed by Krumo et al.[32] The matrix did not support the fibers in

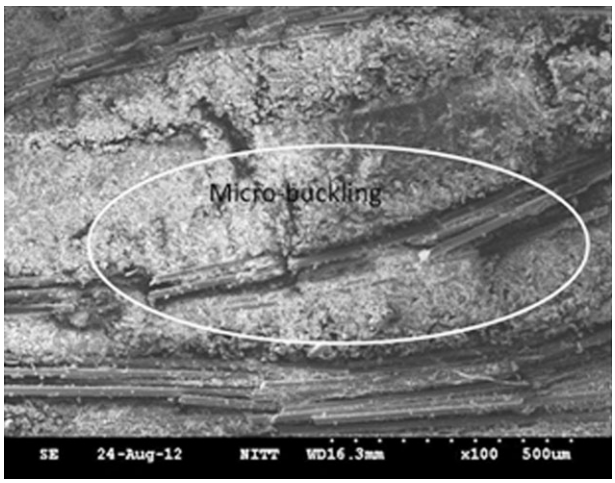

Figure 7. SEM photomicrographs of glass-E after compression testing.

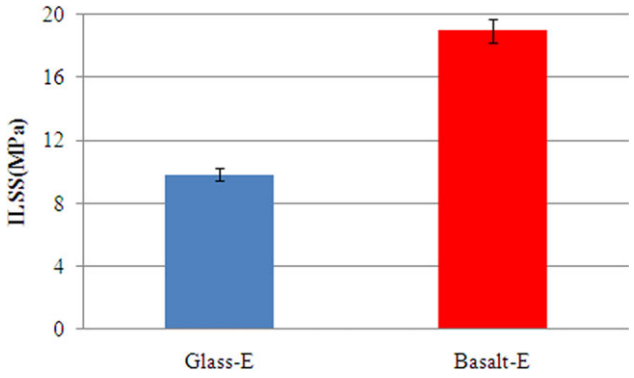

Figure 8. Interlaminar shear strength of the laminated composites. [Color figure can be viewed in the online issue, which is available at wileyonlinelibrary.com.]

glass-E composites, leads to fiber buckle. Formation of micro-buckling leads to local de-lamination and reduce the compression strength for the laminated composites.

Inter-Laminar Shear Strength

The bond strength between the fibre and the matrix resin in the laminated composites was determined by an Inter-laminar shear strength test. Generally in the laminated composites, when the transverse shear load exceeds the inter-laminar shear strength, a de-lamination failure will occur between the layers of reinforcing fibers.

Figure 8 indicates that the value of ILSS of basalt-E is of 48% higher than that of Glass-E. This confirms that a good bond exist between the basalt fiber and epoxy resin. The compression test results also show the same. The better interface between the fiber and matrix can bond the fibers tightly to endure the bigger compression load.[33] If voids are formed in the composites, they deteriorate the load transfer capability significantly, due to the stress concentration around them. High void formation between the epoxy and glass fabric leads to the decrease in inter-laminar shear strength of the glass-E composites. The high value of inter-laminar shear strength of basalt-E composites was due to the lower void content evidenced from Table II.

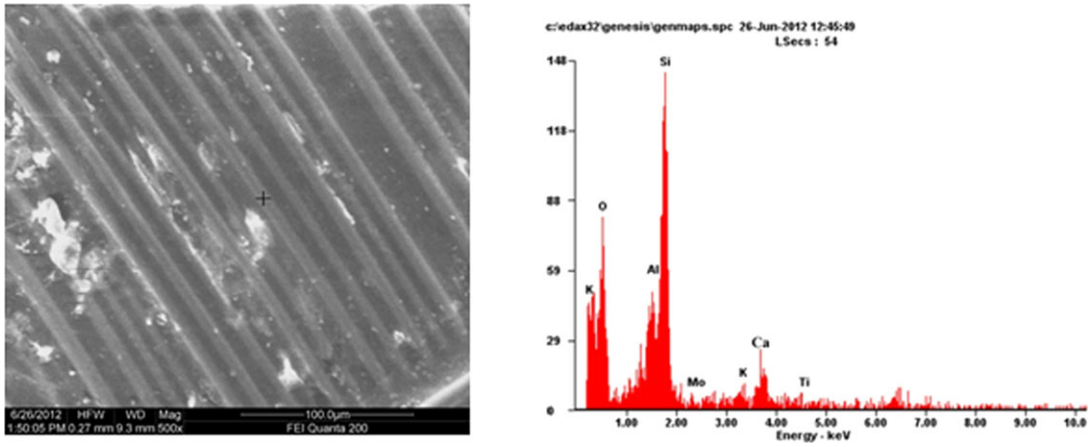

Figure 9. SEM image of Glass-E composites; EDS spectra shows the elemental composition. [Color figure can be viewed in the online issue, which is available at wileyonlinelibrary.com.]

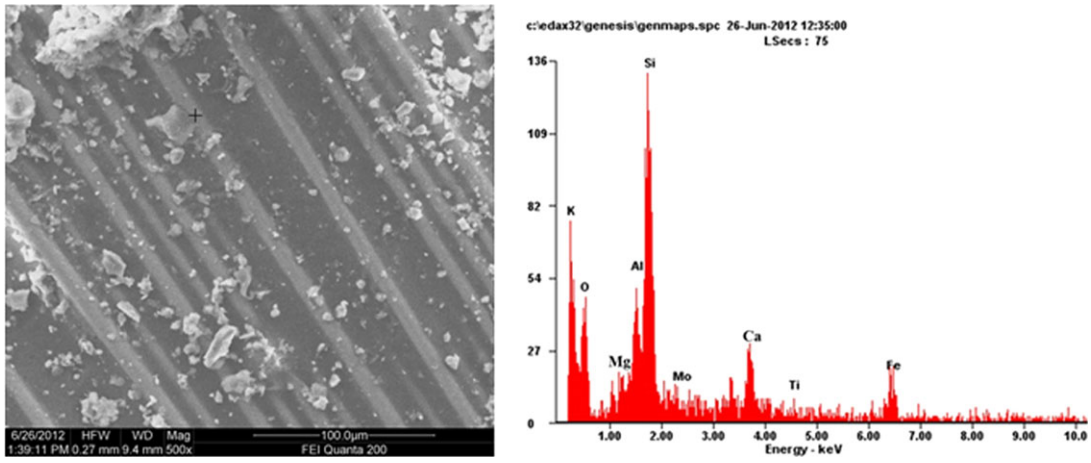

Figure 10. SEM image of Basalt-E composites; EDS spectra shows the elemental composition. [Color figure can be viewed in the online issue, which is available at wileyonlinelibrary.com.]

Table III. Chemical Compositions of Glass Fibers (wt %)

Element	O	Al	Si	K	Ca	Ti	Mo
Wt (%)	45.76	9.91	31.14	1.21	10.05	0.47	1.45

Table IV. Chemical Compositions of Basalt Fibers (wt %)

Element	O	Al	Si	K	Fe	Ti	Ca	Mo	Mg
Wt (%)	44.28	9.91	26.65	1.67	9.97	0.44	0.7	4.50	1.93

Hardness

From Table II, Basalt-E composite exhibits 17.3% higher hardness than Glass-E composites. The high hardness may be due to the good bonding between the basalt and epoxy which transmits the entire load to the strong and high modulus reinforced basalt fibers.

Energy Dispersive X-Ray Spectroscopy

The surface morphologies shown in Figures 9 and 10 of the glass and basalt fibers were characterized using a Hitachi S- 4700 field emission gun scanning electron microscope (FEGSEM) equipped with an energy dispersive X-ray spectrometer (EDS), manufactured by EDAX Inc., US). EDS is accurate for the presence of elements qualitatively and it may be the same quantitatively also. The detection error of EDS is within the limits of 2% in all cases irrespective of spot size, magnification and current.

The EDS analysis is done to indicate the composition difference between the basalt fiber and glass fiber. The obtained values of chemical composition of glass-E and basalt-E composites are given in Tables III and IV.

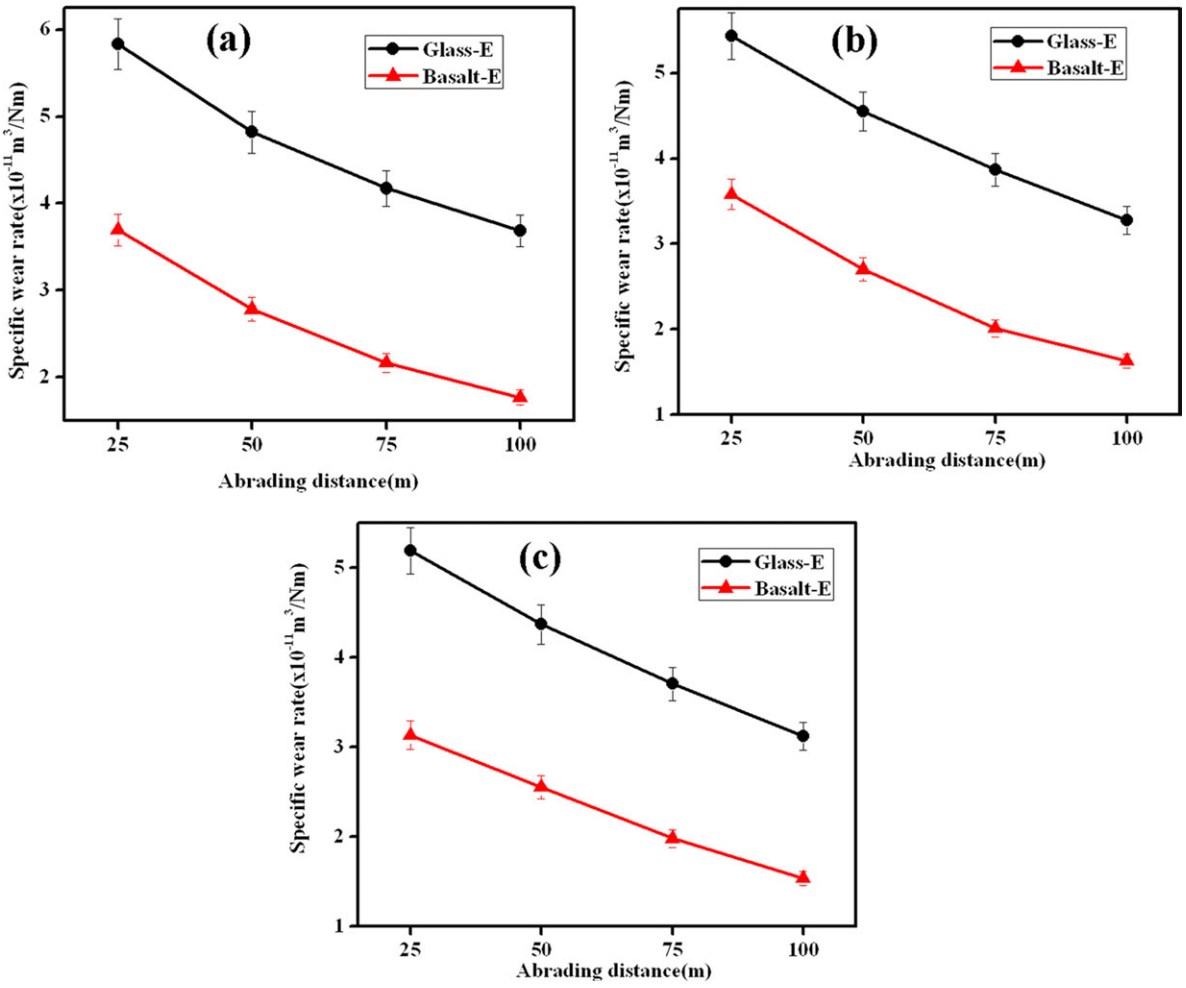

Figure 11. Specific wear rate vs. abrading distance for (a) load = 5 N (b) 10N (c)15 N. [Color figure can be viewed in the online issue, which is available at wileyonlinelibrary.com.]

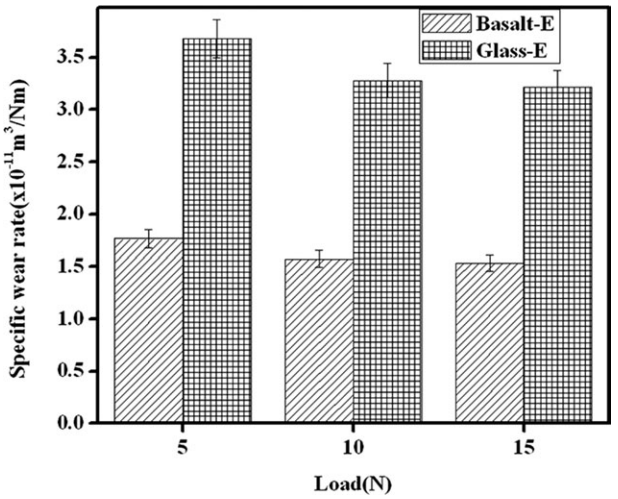

Figure 12. Specific wear rate vs. load for laminated composites for abrading distance of 100 m.

The chemical composition of the basalt fiber is more complex than that of the E-glass, and mainly distinguishes by its content of iron as oxides. The element Fe existing as Fe_2O_3 and FeO in basalt fiber results in the color and density distinction between basalt fiber and glass fiber. The value of density of basalt is high compared with glass due to the presence of high atomic weight of element Fe. The EDS analysis reveals that basalt contains all ingredients naturally whereas in fiber glass special properties are obtained by addition of certain minerals. The presence of iron oxides in the basalt structure gives it a golden brown color and the fiber glass is translucence.

Specific Wear Rate

The magnitude of inverse of specific wear rate determines the intensity of abrasive wear resistance of the composites. The effect of different loads as a function of abrading distance on specific wear rate of glass-E and basalt-E composites is shown in Figure 11. Specific wear rate of the fiber-reinforced composites was in the range of (1–5) $\times 10^{-11} m^3/Nm$. An increase in the abrading distance results in a linear trend for all the applied loads of the composites. Similar results were obtained by various researchers for bi-directional fabrics-reinforced composites.[11,36,37] For low abrading distance maximum wear rate was observed for all the loads tested, due to the freshness of the presence of grits in the SiC grit paper. With an increase in abrading distance, the wear rate decreased gradually because the abrasive grits become smooth and less effective.

The basalt-E composite showed the minimum wear rate, while the glass-E showed the maximum wear rate. This was attributed to the fact that during abrasion of the composites, first resin comes into contact and is easily worn out. Then fibers come into contact with SiC grits. In the glass-E composites, the exposed glass fibers have less hardness and are easily damaged by the grits. The high hardness and modulus of basalt fabric-reinforced composites are attributed to the presence of Fe which in turn resists the abrasive wear and hence a lower specific wear rate was obtained at all loads.

Wear Property Corelation

Lhymn studied the corelation between applied load and specific wear rate of polymer composites.[34] As per Lhymn equation the specific wear rate decreased with an increase in load. The results agreed well with the presence of basalt-E and glass-E composites (Figure 12).

Table V[35–39] lists the various types of correlations between mechanical property and specific wear rate for FRP composites in the literature. Using Ratner-lancaster plot, various researchers reported mechanical properties (hardness, tensile strength, and elongation) which are responsible for the influence of abrasive wear of continuous, short and long FRP composites. But for bidirectional fabrics composites few researchers explore the correlation between mechanical properties and specific wear rate. Among the various mechanical properties the role of Inter-laminar Shear Strength (ILSS) and Young's modulus (E) in controlling abrasive wear of composites were reported by Tsukizoe and Ohmae.[35] Good linear co-relation was obtained between $(ILSS \times E)^{-1}$ vs. specific wear rate for bi-directional carbon fabric-reinforced polyethermide composites.[36] Hence this co-relation has been justified to explain the better abrasive wear resistance of basalt-E than glass-E composites. In the present work the reciprocal of the product of ILSS and E values were calculated as 2.7131×10^{-06} and 1.521×10^{-5} for basalt-E and glass-E composites respectively. It was interesting to note that the higher values of ILSS and E showed the lowest specific wear rate, because higher ILSS values provided maximum resistance to the fiber pull out from the matrix during wear.

Wear Mechanism of Laminated Composites

The wear of polymer composites proceeds by the following sequence

Table V. Literature Review on Mechanical Property Correlation vs. Specific Wear Rate

Sl. no	Resin	Fiber reinforced	Property correlated for specific wear rate	Ref.
1	Epoxy,polyester, PTFE	Carbon fiber, E-glass fiber, aramid fiber	Young's modulus, ILSS	35
2	Polyetherimide	Carbon fabric	ILSS, elastic modulus	36
3	Polyetheretherketone (PEEK)	Short carbon fiber	Impact resistance, flexural modulus Flexural strength	37
4	Polyester	Chopped fibers	Compression, hardness	38
5	Polyetherimide	Carbon fabric	Tensile strength, ILSS	39

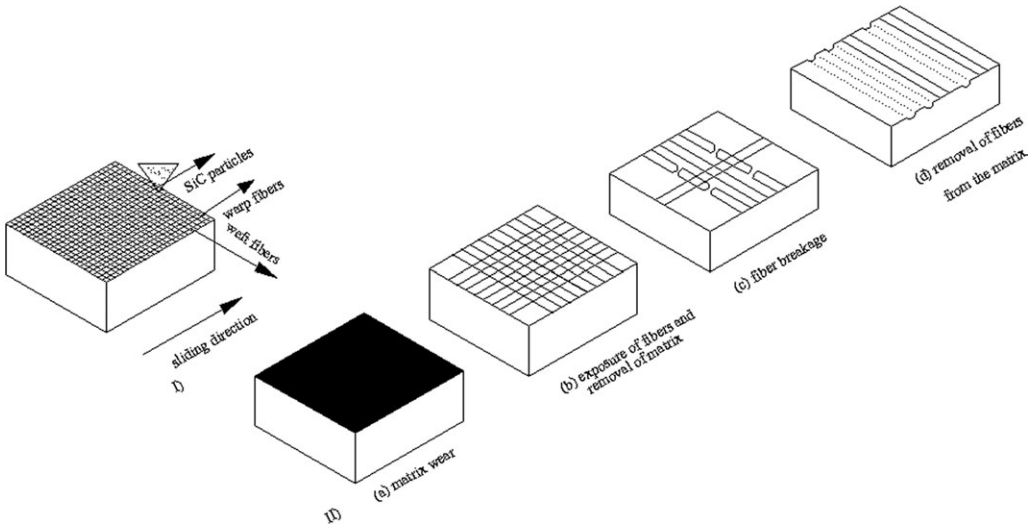

Figure 13. (I) Orientation of laminated composites before wear. (II) Schematic illustration demonstrates the wear process in sequential steps for FRP composites.

1. Matrix wear.
2. Exposure of reinforced fibers followed by fiber micro-cracking and micro-cutting.
3. Fiber breakage.
4. Removals of fibers from the matrix, accounting for wear leaving behind cavities of appropriate size.

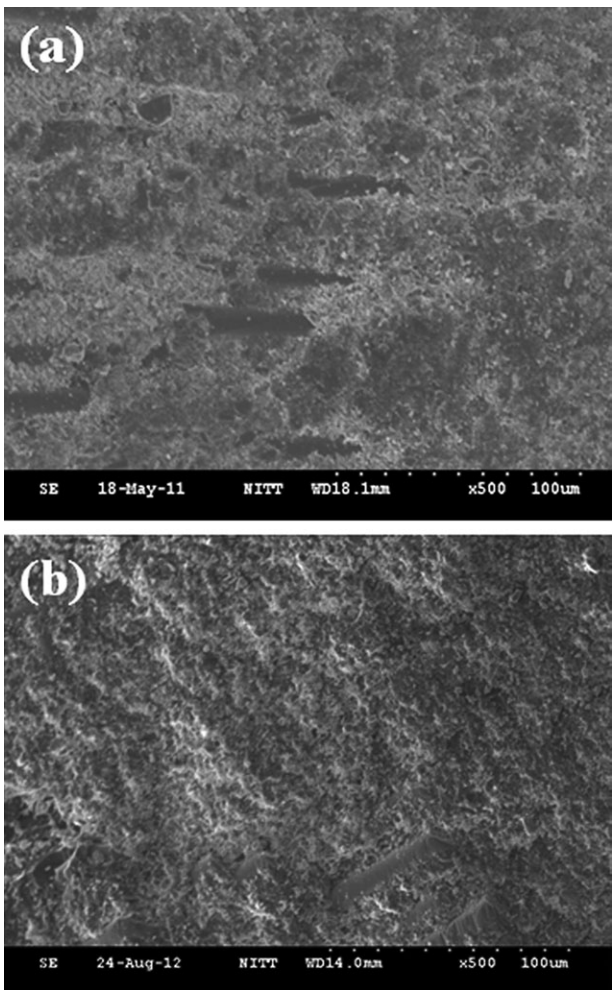

Figure 14. SEM images of worn surface of (a) glass-E (b) basalt-E composite at 5*N* load, 100 m abrading distance.

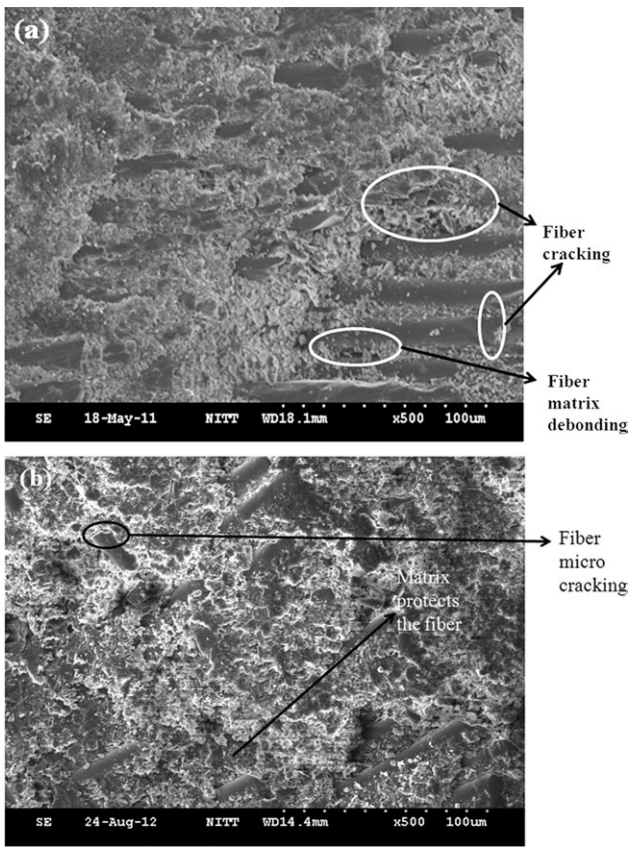

Figure 15. SEM images of worn surface of (a) glass-E (b) basalt-E composite at 10*N* load, 100 m abrading distance.

Applied Polymer SCIENCE

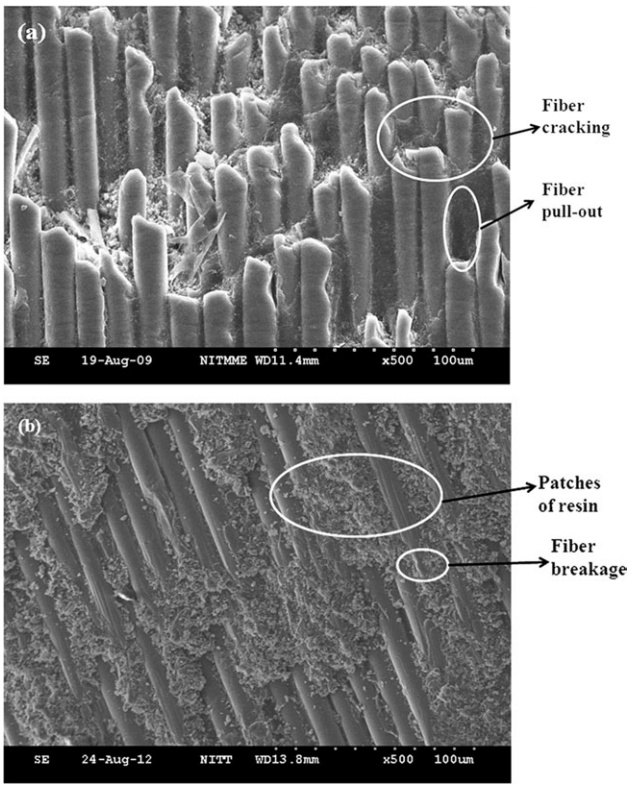

Figure 16. SEM images of worn surface of (a) glass-E (b) basalt-E composite at 15*N* load, 100 m abrading distance.

The worn out surface of the composites was studied using SEM, in order to understand the above mentioned wear mechanism. Figure 13 [steps (a) to (d)] demonstrates the schematic illustrations of the abrasive wear of the FRP composites.

SEM images of the worn surfaces of glass-E and basalt-E composites at 5 N load, 100 m abrading distance are shown in Figure 14(a,b), respectively. Figure 14(a) shows the effect of load on the damage of matrix and breakage of fiber for glass-E composites. Exposure of glass fibers and fiber cracks are visible at surface of the glass-E composite. Minimum amount of matrix was removed from the worn surface of the basalt-E composite compared to glass-E composite. Consequently exposure of fibers is less for basalt-E composites [Figure 14(b)].

The better bonding characteristics of basalt fibers with epoxy[40] enhance low matrix wear and fiber damage to the reinforced composites. Fiber breakage for glass-E composites has increased significantly at 10N load [Figure 15(a)]. Broken glass fibers are exposed due to less fiber-matrix adhesion. Generally glass fibers are brittle in nature and fractured easily due to the applied load.[41] Also the damage to the glass fibers in various forms such as fiber cracking, fiber micro cutting, breakage and extent of deterioration in fiber matrix de-bonding are also observed. Figure 15(b) shows an adequate amount of matrix has held the basalt fibers firmly and this lead to the transfer of load from matrix to the fibers. At few locations, micro-cracking of fibers are visible on the surface of the composites. The damage of matrix and fiber is less in basalt-E composites as compared to glass-E composites under the load of 10N. The basalt fibers remained attached to the epoxy due to plastic deformation to a high degree, when applied load is imposed on them. Hence, the basalt-E composites exhibited a relatively lower wear rate than glass-E composites.

When load increased from 5 N to 15 N the amount of fiber damages increased, which was responsible for high volume loss of glass-E composites. At high load, fibers are subjected to shear force when the grits slides over them, resulting in the removal of the matrix material. So the entire load is carried by the fibers. In the case of glass-E composites, fibers are unable to withstand at high load, which leads to breakage. Severe damage to the glass fibers are examined from Figure 16(a), which supports its lowest wear resistance. Few fractured fibers remain attached to the composite surface which was also observed. Similar results were obtained by Navin Chand et al.[42]

Also SEM images reveal more fiber pull out on the abraded surfaces of the glass-E composites. Because when higher loads are acting on composite,the fibers get detached from the resin and tends to more breakage of fibers, resulting in pieces followed by peeling-off or pullout of fibers from the matrix.[35] The features of surfaces basalt-E composites in Figure 16(b). shows the microcracking of fibers and lower fiber consumption.Some patches of resin covering the fibers are also visible in the top

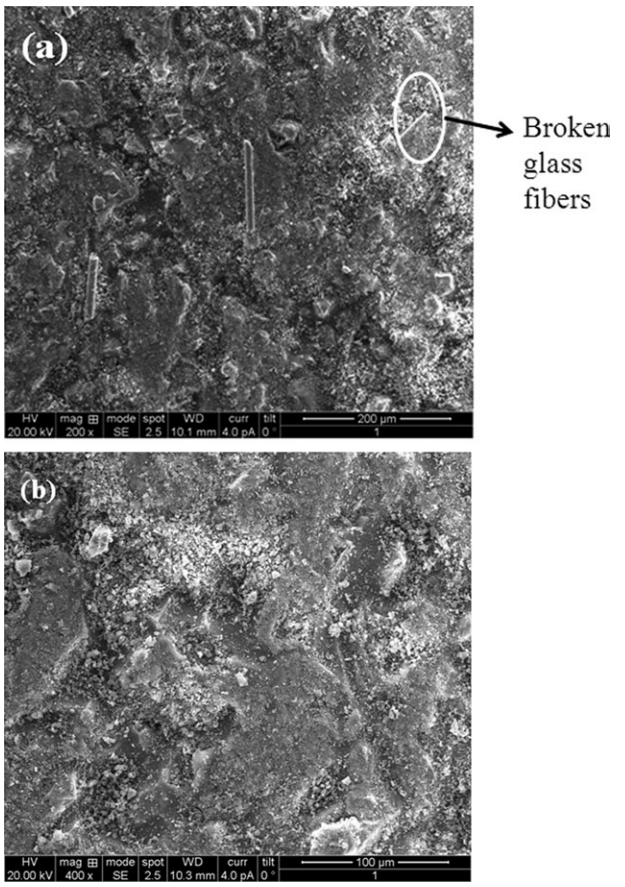

Figure 17. SEM images of SiC papers worn against (a) glass-E and (b) basalt-E composite at 15*N* load, 100 m abrading distance.

portion of the SEM image,while these were not observed in glass-E composites. The good bonding between fibers and matrix of the basalt-E composites has a positive influence on the abrasive wear behavior. It is observed that some fiber ends break off, while the remaining parts of the fibers stay embedded in the matrix. This is why the fibers in these composites did not pullout easily, therefore the damage to the fibers was low.The adhesive interaction of basalt fibers is stronger than that of glass fibers, due to the high content of iron oxides and Fe^{+2} and Fe^{+3} iron ions, respectively.[43] This increases the high co-ordination ability between basalt fibers and resin. Thus better bonding was observed between matrix and basalt fibers in basalt-E composites, at all loads. These resulted to less fiber breakage and fibers pull out for the reinforced composites. It is clear that the basalt-E composite have exceptional wear resistance characteristics, than glass-E composite. Figure 17(a,b) shows the image of worn SiC papers of glass-E and basalt-E composites respectively.SEM image 17(a) indicated that some broken glass fibers, as wear debris, stick to the surface of the worn SiC paper. This supports low wear resistance of the glass-E composites due to the fibers peeling out from the matrix on account of less adhesion. While SEM image at high magnification [Figure 17(b)] shows hardly any wear debris of basalt fiber/matrix supporting good wear resistance of this composite.

CONCLUSIONS

The following conclusions were drawn from the experimental study on two body abrasive behavior of Basalt-E and Glass-E composites.

A good bonding between basalt fibers and matrix has a positive influence on the abrasive wear behavior.

Basalt fibers prove to be effective in increasing the wear resistance of the composites.

Glass-E composites are detrimental to abrasive wear due to poor bonding between fibers and resin.

Mechanical properties determined by inter-laminar shear strength and Young's modulus test exert a notable impact on the specific wear rate of the composites. The increased inter-laminar strength of basalt-E composites leads to high wear resistance.

The analysis of worn surfaces of glass-E composites reveals matrix wear, breakage of fiber, and fiber pull-out due to the abrasive wear of the SiC particles.

The outcome of the results suggested that basalt fabric-reinforced epoxy composites has the possibile application in abrasive wear situation, owing to its better abrasive wear resistance and good mechanical properties. However, this situation may differ from other resins.

REFERENCES

1. Friedrich, K.; Lu, Z.; Hager, A. M. *Wear* **1996**, *190*, 139.
2. Stachowiak, W.; Batchelor, A. W. Engineering Tribology; Elsevier: Amsterdam, **1993**; Chapter 3, p 92.
3. Friedrich, K. Friction and Wear of Polymer Composites; Elsevier: Amsterdam, **1986**; p 137.
4. Chattopadhyay, R. Surface Wear: Analysis, Treatment, and Prevention; ASM International: Materials Park, **2001**; p 116.
5. Blau, J. ASM Handbook; Friction, Lubrication, and Wear Technology; ASM International: Materials Park, **1992**; Vol.*18*, p 184.
6. Neale, M. J.; Gee, M. Guide to Wear Problems and Testing for Industry; William Andrew Publishing: New York, **2001**; Chapter 2, p 8.
7. Standard terminology relating to wear and erosion; Annual Book of Standards, ASTM, **1987**; p 243.
8. Buchanan, V. E.; Shipway, P. H.; McCartney, D. G. *Wear* **2007**, *263*, 99.
9. Sampathkumaran, K.; Seetharamu, P.; Vynatheya, S.; Murali, S.; Kumar, R. K. *Wear* **2000**, *237*, 20.
10. Sampathkumaran, K.; Seetharamu, S.; Thomas, P.; Janardhana, M. *Wear* **2005**, *259*, 634.
11. Suresha,B.; Chandramohan, G.; Sadananda Rao,P. R.; Sampathkumaran, P.; Seetharamu, S. *J. Reinf. Plast. Comp.* **2007**, *26*, 565.
12. Sandhyarani, B.; Satapathy, A. *Mater. Des.* **2009**, *30*, 2841.
13. Basavarajappa, S.; Ellangovan, S.; Arun, K. V. *Mater. Des.* **2009**, *30*, 2670.
14. Patnaik, A.; Satapathy, A.; Sandhyarani, B. *Malay. Poly.* **2010**, *5*, 37.
15. Basavarajappa, S.; Ajith, G.; Joshi; Arun, K. V.; Praveen Kumar, A.; Prasanna Kumar, M. *Polym.-Plastics Technol.* **2010**, *49*, 8.
16. Mohan, N.; Natarajan, S.; Kumaresh Babu, S. P. *Mater. Des.* **2011**, *32*, 1704.
17. Suresha, B.; Shiva Kumar, K. N. *Mater. Des.* **2009**, *30*, 2056.
18. Friedrich, K. Wear Model for Multiphase Materials and Synergistic Effect in Polymeric Hybrid Composites; Wood Head Publishing: Cambridge, **1993**; Chapter 6, p 147.
19. Gay, D; Hoa, S. V.; Tsai, S. W. Composite Materials: Design and Applications; CRC Press: New York, **2003**; Chapter 3, p 41.
20. Czigany, T. *Express Polym. Lett.* **2007**, *1*, 59.
21. Witteka, T.; Tanimoto, T. *Adv. Compos. Mater.* **2009**, *18*, 167.
22. Kim, Y.; Yang, D.; Yoon, S.; Lee, B. W.; Park, S.; Kim, D.; Bae, C. W.; Moon, K. *Adv. Sci.Lett.* **2011**, *4*, 1633.
23. Kukureka, S. N.; Hooke, C. J.; Rao, M.; Liao, P.; Chen, Y. K. *Tribol. Int.* **1999**, *32*, 107.
24. Bashtannik, P. I.; Ovcharenko, V. G.; Boot, Y. A. *Mech. Compos. Mater.* **1997**, *33*, 299.
25. Czigány, T. *Mater. Sci. Forum.* **2005**, *473*, 59.
26. Czigany, T.; Vad, J.; Poloskei, K. *Periodica Polytechnica Mech. Eng.* **2005**, *49*, 3.
27. Wei, B.; Cao, H.; Song, S. *Mater. Sci. Eng. A.* **2010**, *527*, 4708.
28. Lopresto, V.; Leone, C.; De lorio, I. *Compos. Part B-Eng.* **2011**, *42*, 717.
29. Wei, B.; Cao, H.; Song, S. *Corros. Sci.* **2011**, *53*, 426.

30. Lubin, G. Handbook of Fiber Glass and Advanced Plastics Composites; Van Nostrand Reinhold Company: New York, **1969**; Chapter 3, p 46.
31. Krumova, M.; Klingshirn, C.; Haupert, F.; Friedrich, K. *Compos. Sci. Technol.* **2001**, *61*, 557.
32. Yanga, B.; Kozeya, V.; Adanurb, S.; Kumar, S. *Compos: Part B-Eng.* **2000**, *31*, 715.
33. Deak, T.; Czigany, T.; Tamas, P.; Nemeth, C. *Express Polym. Lett.* **2010**, *4*, 590.
34. Lhymn, C. *Wear* **1987**, *120*, 1.
35. Sukizoe, T.; Ohmae, N. *Fiber Sci. Technol.* **1983**, *18*, 265.
36. Bijwe, J.; Rattan, R.; Fahim, M. *Tribol. Int.* **2007**, *40*, 844.
37. Zhang, Z.; Breidt, C.; Chang, L.; Friedrich, K. *Tribol. Int.* **2004**, *37*, 271.
38. Yousif, B. F.; Tayeb, E. I. *Tribol. Int.* **2010**, *43*, 2365.
39. Bijwe, J.; Rattan, R. *Wear* **2007**, *262*, 749.
40. Liu, Q.; Shaw, M. T.; Parnas, R. S.; McDonnell, A. M. *Polym. Compos.* **2006**, *27*, 41.
41. Suresha, B.; Chandramohan, G.; Renukappa, N. M.; Siddaramaiah, J. *Appl. Polym. Sci.* **2007**, *103*, 2472.
42. Chand, N.; Naik, A.; Neogi, S. *Wear* **2000**, *242*, 38.
43. Dalinkevich, A. A.; Gumargalieva, K. Z.; Marakhovsky, S. S.; Soukhanov, A. V. *J Nat. Fibers.* **2009**, *6*, 248.